An ionospheric convection signature of antiparallel reconnection

Iain J Coleman, Gareth Chisham, Mike Pinnock, Mervyn P Freeman

Abstract

The issue of the location of reconnection sites on the dayside magnetopause is as yet unresolved. There are two main hypotheses: subsolar reconnection and antiparallel merging. Using a magnetosphere-ionosphere mapping model, we show that antiparallel merging sites have a distinctive ionospheric footprint when IMF B_z is southward and $|B_y| \sim |B_z|$, with a gap in the merging line near noon which becomes significant close to midwinter. We go on to predict that this near-noon gap will result in a characteristic ionospheric flow signature, with equatorward flow in the noon sector and poleward flow in the duskward and dawnward regions. This convection signature is inconsistent with subsolar merging, and is a critical test of the antiparallel merging hypothesis. Finally, we discuss a period, close to midwinter, when the IMF conditions were appropriate for our model, and show that the ionospheric convection pattern was similar to that predicted by antiparallel reconnection.

1 Introduction

The issue of where reconnection occurs on the dayside magnetopause is still unresolved. There are two main hypotheses: sub-solar merging, in which reconnection takes place always at the sub-solar point (Gonzalez and Mozer, 1974), and anti-parallel merging (Crooker, 1979), which states that reconnection takes place on those regions of the magnetopause where the magnetosheath and magnetopause fields are oppositely directed. Our aim is to make a quantitative connection between magnetopause merging sites and observations of ionospheric signatures of reconnection, and thus to develop a critical test of the anti-parallel merging hypothesis.

Ionospheric measurements give us an image of the large-scale features of the dayside magnetopause. Since the distinction between subsolar and antiparallel reconnection concerns just such a large-scale feature, there is a strong motivation for addressing this issue via ground-based measurements. This paper sets out the distinctive features of antiparallel merging which can be seen in magnetosphere-ionosphere mapping.

We use the mapping method set out in Coleman et al. (2000). This is based upon the Tsyganenko 96 magnetospheric field model (Tsyganenko, 1995; Tsyganenko and Stern, 1996), and incorporates field line draping. Our model of anti-parallel reconnection sites follows that of Luhmann *et al.* (1984), albeit in a slightly simplified fashion.

We go on to predict a characteristic convection signature which can clearly distinguish between antiparallel and subsolar reconnection. Our treatment of ionospheric convection is analytic, and is based on the approach of Freeman et al. (1991). This convection model

is therefore not fully integrated with the mapping model: rather, it captures the gross features of the mapping results in a somewhat simplified fashion.

Our approach can be regarded as complementary to that of Maynard et al. (1995). In that paper, the statistical convection patterns of Heppner & Maynard (1987) were mapped into the magnetosphere. Our treatment of convection, which relies on a purely analytic model, brings out small-scale, seasonally-dependent phenomena which are not present in a statistical model, although the latter is a more realistic representation of the typical behaviour of the system.

2 The mapping model

As set out in Coleman et al. (2000), our mappig model has three main components: field line draping in the magnetosheath, reconnection rate and magnetospheric magnetic field. For the sake of simplicity, we have used the "perfect draping" approximation: that is, the magnetosheath field is everywhere tangential to the magnetopause. This is a good approximation on the dayside, becoming less realistic further towards the tail. For our reconnection model, we adopt the anti-parallel merging hypothesis: reconnection occurs in those regions where the magnetosheath and magnetosphere field are oppositely directed. Following Luhmann *et al.* (1984), we use the criterion that the fields must be within 10° of being anti-parallel. Finally, we use the Tsyganenko 96 magnetospheric field model for the field-line tracing from the magnetosphere to the ionosphere. There is no time-dependence in the model.

The methodology is straightforward. First, we specify the solar wind conditions (B_y, B_z, and dynamic pressure), D_{st} and the epoch (year, day and UT), as required by the Tsyganenko 96 model. Then we discretise a region on the magnetopause from the subsolar point to approximately 25 Re tailward of Earth, beyond which the perfect draping approximation is unlikely to be applicable. The limit to this approximation will depend upon the solar wind parameters: analytic modelling of the magnetosheath field (Kobel and Flückiger, 1994) indicates that our chosen cutoff is reasonable for an IMF with no x component. At each point on this grid, we calculate the magnetic shear ϕ. Where the merging criterion is fulfilled (here, $cos(\phi) \leq -0.98$), the field line is traced to the ionosphere. The end result is an array of points in the ionosphere (corrected geomagnetic latitudes and longitudes) with their associated merging angles and the GSM coordinates of the starting point on the magnetopause. This is used to construct the maps shown in the following sections.

2.1 Magnetopause regions

Rodger *et al.* (2000) argue, following La Belle-Hamer *et al.* (1995), that quasi-steady reconnection can only occur within the region of sub-Alfvénic magnetosheath flow (between the subsolar point and the Alfvénic boundary), and that only transient reconnection is possible in the super-Alfvénic regime. In mapping the magnetopause merging line to the ionosphere, we are primarily interested in the quasi-steady-state reconnection that can occur in the sub-Alfvénic magnetopause region, and we assume that most of the reconnection potential generated will appear in this region.

The location of the Alfvénic boundary depends mainly upon the velocity of the solar wind. We have adapted the approach of Cowley and Owen (1989), who calculated that this boundary would lie at a distance of 6.8 R_e along the magnetopause from the subsolar point, based on a typical solar wind velocity of 500 kms^{-1}. Following the calculation in

Coleman *et al.* (2000) the x-coordinate x_a of the Alfvénic boundary in the GSM system is $x_a = 6.2\ R_e$, for our chosen model parameters.

3 Model results

We discuss two epochs: 2300 UT on 21 March (dipole tilt 0°) and 0500 UT on 21 December (dipole tilt −34°). In both cases, we have prescribed a moderate southward value for the IMF B_z component: $B_z = -3\ nT$. We have then modelled the reconnection sites and ionospheric footprints for the $B_y = 3\ nT$ case. This is a typical value for IMF B_y (Leonard *et al.* (1995)) . Dst and solar wind pressure remain fixed at typical values. Specifically, $D_{st} = -20\ nT$ and $P_{dyn} = 2.5\ nPa$.

3.1 Magnetopause maps

Figures 1 and 2 show the extent of the antiparallel regions on the magnetopause, for the two epochs considered in this paper.

The projection is in the $y - z$ GSM plane. The '10' contours show the boundaries of the merging regions (where the terrestrial and interplanetary fields are within 10° of antiparallel). The ellipse shows the Alfvénic boundary.

Figure 1 shows the antiparallel regions at equinox. They form two 'horns', one above and one below the equator. In this B_y positive case, the northern horn is on the dusk side, and the southern horn is on the dawn side: for B_y negative, the opposite is true. There is a difference of about a factor of two in the field-aligned distance from the horns to the ionosphere in a given hemisphere.

Figure 2 shows the situation at the December solstice. In December, the tilt of the Earth's dipole moved the southern horn towards the equator, while shifting the northern

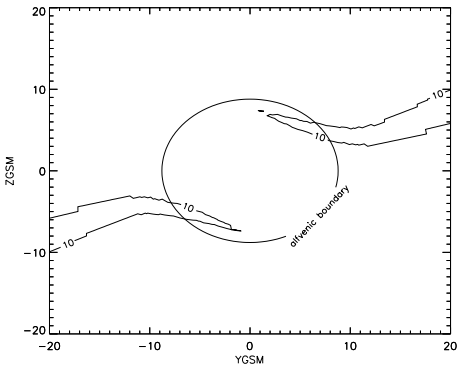

Figure 1: Magnetopause maps in the $y - z$ GSM plane for the northern vernal equinox, northern winter and northern summer, with IMF $B_z = -3\ nT$, $B_y = 3\ nT$. The '10' contour marks the region where the terrestrial and interplanetary fields are within 10° of being anti-parallel. The elliptical contour marks the Alfvénic boundary.

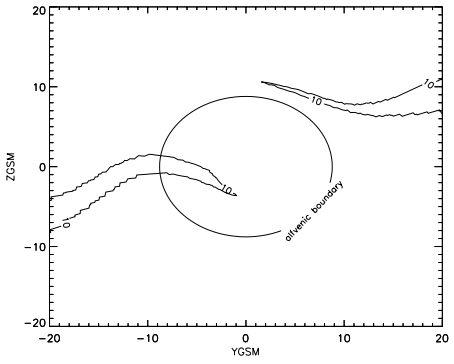

Figure 2: Magnetopause maps in the $y - z$ GSM plane for the northern winter and northern summer, with IMF $B_z = -3\ nT$, $B_y = 3\ nT$.

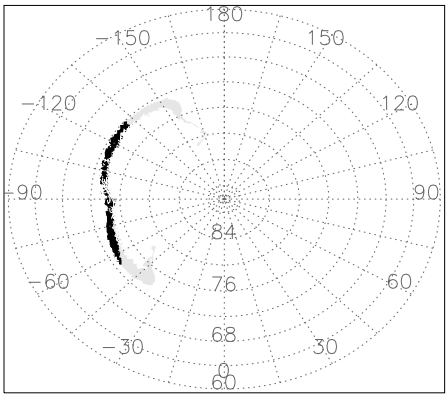

Figure 3: Merging line at the northern vernal equinox for 2300 UT. These maps show where the antiparallel region on the magnetopause maps to the ionosphere, in the northern hemisphere, in magnetic latitude and longitude. The dark shading corresponds to the sub-Alfvénic region, the light shading to the super-Alfvénic region. Solid lines indicate where the dayside-nightside boundary at the flanks of magnetopause maps to in the ionosphere.

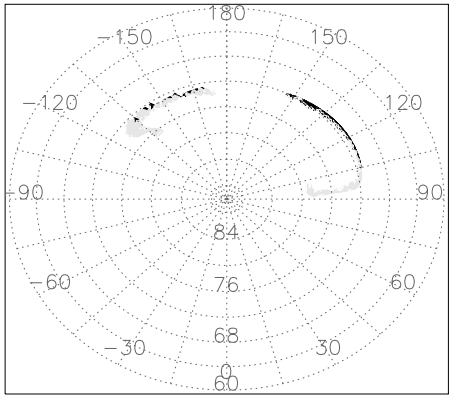

Figure 4: Merging regions at midwinter in the northern hemisphere for 0500 UT. The coordinate system and greyscale shading scheme are as in Fig. 3.

horn away from the equator and out of the sub-Alfvénic region.

3.2 Ionospheric maps

Figures 3 and 4 show where the anti-parallel region on the magnetopause maps to in the northern ionosphere, in corrected geomagnetic latitude and longitude. The greyscale coding indicates whether the sub- or super-Alfvénic magnetopause region is mapping to that particular point in the ionosphere. The darker shading corresponds to the subsolar, sub-Alfvénic region, the lighter shading shows the super-Alfvénic region.

At equinox, there is very little separation between the footprints of the two merging regions. Indeed, the footprints merge to form a single x-line, the sub-Alfvénic portion of which spans 5 hours of MLT (Figure 3). This single x-line would be expected from sub-solar merging as well as antiparallel reconnection. These two footprints do map to well-separated regions of the magnetopause: one above the equator, one below. For practical purposes, therefore, there is a single x-line along which the magnetopause-ionosphere travel time for injected particles and Alfvén waves varies discontinuously.

At midwinter (December 21), the near-noon gap is at its maximum extent (Figure 4), reaching a width of ~ 2 hours MLT. The overall width of the footprint is also at a maximum, spanning 8 hours from end to end, albeit discontinuously. This is mainly caused by the flaring out of the field lines on the magnetopause close to noon in the winter hemisphere, due to their experiencing much lower solar wind pressure than in the summer hemisphere (Coleman et al., 2000).

Thus, the gap between the antiparallel footprints is only significant near midwinter. The

next section will deal only with the midwinter case, showing the characteristic convection pattern that we predict for this situation. In other seasons, the gap is very small. However, there is still a discontinuity along the ionospheric x-line, because the two merging regions on the magnetopause are well-separated, and in summer are in quite different physical regimes.

4 Convection signatures of antiparallel merging

We can model the effects of the broken x-line on ionospheric convection patterns with a somewhat idealised analytical model. In this paper, we use a modified version of the Freeman and Southwood (1988) model.

The model assumes that the ionosphere is in a steady state and of uniform conductivity, with a vertical magnetic field. Requiring the polar cap boundary to be circular, we follow exactly the same procedure as is set out in the appendix of Freeman et al. (1991). The only new element in the present model is that we impose a constant eastward reconnection electric field along two segments of the polar cap boundary. This model does not consider B_y tension effects (Cowley 1982), which would break the symmetry of the results in the next section. A future development of the model will address that factor.

At most times of year, there is little to distinguish the convection pattern of a broken x-line from that of an unbroken x-line. This is simply because the gap is so small compared to the width of the x-line that it has no significant effect. Near the winter solstice, however, this is not the case. At this time, the gap around noon can be greater than 1 hour wide in MLT. This is an effect of the mapping geometry: field lines mapping to the winter hemisphere experience less solar wind ram pressure than those mapping to the summer hemisphere, and are thus able to expand into a greater volume of the magnetosphere. The result is a wider ionospheric footprint in general, and a wider near-noon gap in particular.

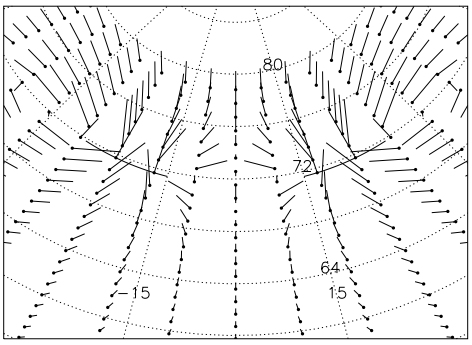

Figure 5: Model convection velocity vectors, in a geomagnetic coordinate system with magnetic noon at 0° magnetic longitude. The merging lines are indicated by thick solid curves.

Figure 5 shows the model convection pattern for the case of a broken x-line with a 2-hour gap. The two parts of the x-line are each 20° wide, and the potential difference along each section is the same. This is an idealised representation of the midwinter case (Figures 8 and 9).The overall configuration is symmetrical about noon. There is strong poleward flow across both portions of the x-line, but in the gap region the flow is *equatorward* at about 72° latitude. There is a stagnation zone in the noon sector, within the polar cap at around 74° latitude, where the transition between equatorward and poleward flow occurs.

This can be understood most simply by considering the end points of the two portions of the x-line, which also form the end points of the gap region. These are the footpoints of

two vertical, oppositely-directed field-aligned currents. Therefore they give rise to approximately circular equipotentials, with plasma flowing along these equipotentials in opposite senses.

This convection feature is the distinguishing feature of antiparallel merging. It is difficult to see how subsolar merging could mimic such a feature – under steady state conditions, at any rate. All the modelling in this paper assumes that the solar wind is at least quasi-steady, and the resulting predictions only apply when this assumption is valid.

5 Testing the antiparallel merging hypothesis with ground-based radar

The convection pattern described in the previous section is a clear and distinctive signature predicted for antiparallel merging. This enables us to make the following prediction. If the antiparallel merging hypothesis holds true, then close to midwinter, under approximately steady IMF conditions with B_z southward and $|B_y| \sim |B_z|$, observations of the cusp ionospheric flow will show two regions of enhanced poleward flow either side of noon, with equatorward flow in the noon sector.

This is a clear and testable prediction. It does rely on the IMF conditions being appropriate for an extended time interval, during a window of a few weeks either side of midwinter. This is not a common occurrence, but neither is it so rare as to be unobservable in practice. Given those conditions, and good coverage of the cusp flow pattern, the presence or absence of this convection feature will confirm or deny the antiparallel hypothesis.

In the next section, we present radar data from one day which fits all the above criteria.

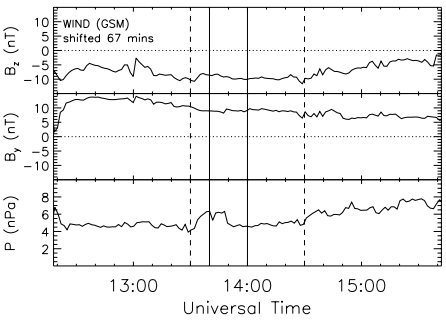

Figure 6: Solar wind data from the WIND spacecraft for December 10, 1997

6 Data Analysis

On December 10, 1997, close to solstice, the near-Earth solar wind was characterised by an extended quasi-steady interval (∼5 hours) during which both the IMF and the solar wind dynamic pressure remained relatively steady. During this interval, IMF B_z was negative and the magnitude of the IMF B_y component was comparable to that of the B_z component which provided a good interval to examine the predictions of the anti-parallel merging hypothesis, as described above.

Figure 6 presents data from the WIND spacecraft during this interval; shown are the IMF B_z and B_y components and the solar wind dynamic pressure. The data have been shifted by 67 minutes to allow for the solar wind propagation time between WIND and the Earth's magnetosphere. This delay time has been calibrated by solar wind observations by the GEOTAIL spacecraft which was located just outside the dawn bow shock. All three of the parameters shown display little variability throughout the interval presented. This would suggest that the magnetopause reconnection scenario is relatively steady throughout this interval.

Figure 7 presents 2-dimensional merged

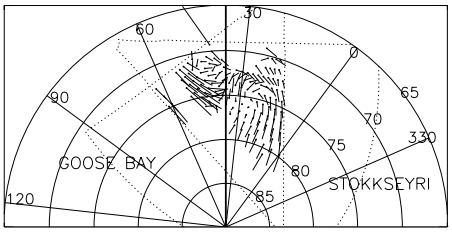

Figure 7: 2-dimensional merged velocity vectors from the Goose Bay and Stokkseyri SuperDARN HF radars. Line-of-sight velocity data from both radars has been averaged over a 20-minute interval (1340-1400 UT).

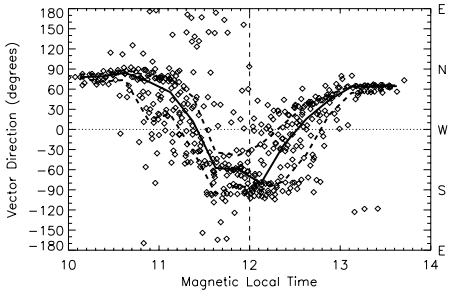

Figure 8: Scatter plot of vector direction against magnetic local time. This includes all the 5-minute vectors observed between 72 and 77 latitude and between 1330 and 1430 UT. The bold line represents the variation of the median of the distribution, and the bold dashed lines represent the upper and lower quartiles.

velocity vectors from the Goose Bay and Stokkseyri SuperDARN HF radars.The dotted lines represent the fields-of-view of the Goose Bay and Stokkseyri radars; the vector information is constrained to the overlapping field-of-view. Line-of-sight velocity data from both radars has been averaged over a 20-minute interval (1340-1400 UT; the region enclosed by the solid vertical lines in Figure 6), before being combined to produce the unambiguous merged velocity vectors. Only F-region ionospheric scatter was considered. The interval size was chosen to result in the most comprehensive vector coverage. The bold vertical line represents the location of magnetic local noon at 1350 UT on this day (the centre of the interval). The velocity vector variation displays a distinctive 'S' shape. Post-noon, the vectors are oriented predominantly poleward, turning westward towards magnetic local noon, and then equatorward around noon. Pre-noon, the vectors turn westward again before turning poleward at the earliest magnetic local times.

It is important to determine the stability of this convection pattern and to show that the spatial velocity variations presented are not a result of temporal variations on a timescale less than 20 minutes. To this end, merged velocity vectors were calculated for 5-minute intervals for an hour of data (1330–1430 UT; as shown by the dashed lines in Figure 6) encompassing the 20-minute interval shown. Although none of the 5-minute convection patterns displayed the comprehensive picture of the ionospheric convection shown in Figure 7, combining information from all these 5-minute patterns allows us to investigate the stability of the pattern over the hour studied. Figure 8 presents a scatter plot of vector direction against magnetic local time. This includes all the 5-minute vectors observed between 72 and 77 latitude and between 1330 and 1430 UT. The bold line represents the variation of the median of the distribution (using 15-minute magnetic local time bins). The bold dashed lines represent the upper and lower quartiles of the distribution. This figure illustrates that the vector direction has a clear variation with magnetic local time with the changes matching exactly those presented in the 20-minute velocity vector pattern in Figure7. In particu-

lar, the flow has a predominantly equatorward component within $\sim \pm 30$ minutes of 12 MLT and a predominantly poleward componenet outside this interval. This confirms that this convection feature was approximately stationary in magnetic local time for this hour-long interval.

7 Conclusions

We have shown that the antiparallel merging hypothesis leads to a prediction of a distinctive convection pattern. Crucially, we only expect this convection feature to manifest itself near midwinter, during intervals of quasi-steady IMF with B_z southward and $|B_y| \sim |B_z|$. This pattern consists of poleward flow either side of noon, with equatorward flow in the noon sector. The presence or absence of this pattern under the specified conditions forms a critical test of the antiparallel merging hypothesis.

This is a robust prediction, in that it is not sensitive to the details of the modelling. It is a consequence of having two well-separated merging regions on the dayside magnetopause (a consequence of antiparallel reconnection) and of the fact that field lines in the winter hemisphere are able to flare out more than those in the summer hemisphere (a feature of any realistic magnetospheric field model).

We have identified an interval with appropriate solar wind conditions on December 10 1997. HF radar vectors show a pattern qualitatively similar to that we expect from antiparallel reconnection. Thus we conclude that, on this day, dayside reconnection was taking place on the antiparallel regions of the magnetopause.

References

[1] **Coleman, I. J., M. Pinnock and A. S. Rodger,** *Annales Geophysicae,* **18,** 511, 2000

[2] **Cowley, S. W. H.,** *Re. Geophys. Space Phys.,* **20,** 531

[3] **Cowley, S. W. H., and C. J. Owen,** *Planet. Space. Sci,* **37,** 1461, 1989.

[4] **Crooker, N. U.,** *J. Geophys. Res.,* **84,** 951, 1979.

[5] **Freeman, M. P., and D. J. Southwood,** Planet. Space. Sci, **36,** 509, 1988

[6] **Freeman, M. P., J. M. Ruohoniemi, and R. A. Greenwald,** *J. Geophys. Res.,* **96,** 15735, 1991

[7] **Gonzalez, W. D., and F. S. Mozer,** *J. Geophys. Res.,* **79,** 4186, 1974.

[8] **Heppner, J. P., and N. C. Maynard,** *J. Geophys. Res.,* **92,** 4467, 1987

[9] **Kobel, E., and E. O. Flückiger,** *J. Geophys. Res.,* **99**, 23617, 1994. **Heppner, J. P., and N. C. Maynard,** *J. Geophys. Res.,* **92,** 4467, 1987

[10] **La Belle-Hamer, A. L., A. Otto, and L. C. Lee,** *J. Geophys. Res.,* , **100**, 11875, 1995.

[11] **Leonard, J. M., M. Pinnock, A. S. Rodger, J. R. Dudeney, R. A. Greenwald and K. B. Baker,** *J. Atmos. Terr. Phys., 57,* 889, 1995.

[12] **Luhmann, J. G., R. J. Walker, C. T. Russell, N. U. Crooker, J. R. Spreiter, and S. S. Stahara,** *J. Geophys. Res.,* **89,** 1739, 1984.

[13] **Maynard, N. C., W. F. Denig, and W. J. Burke,** *J. Geophys. Res.,* **100,** 1713, 1995

[14] **Rodger, A. S., I. J. Coleman and M. Pinnock,** *Geophys. Res. Lett.,* , **27** , 1359, 2000.

[15] **Tsyganenko, N. A.,** *J. Geophys. Res.,* **100,** 5599, 1995.

[16] **Tsyganenko, N. A., and D. P. Stern,** *J. Geophys. Res.,* **101,** 27187, 1996.